

Article

Verifying the Mechanical Performance of Cold and Hot Asphalt Mastics Containing Jet Grouting Waste as a Filler

Francesca Russo ¹, Rosa Veropalumbo ^{1,*}, Cristina Oreto ¹, Salvatore Antonio Biancardo ¹,
Francesco Abbondati ² and Nunzio Viscione ¹

¹ Department of Civil, Construction and Environmental Engineering, Federico II University of Naples, Via Claudio 21, 80125 Naples, Italy; francesca.russo2@unina.it (F.R.); cristina.oreto@unina.it (C.O.); salvatoreantonio.biancardo@unina.it (S.A.B.); nunzio.viscione@unina.it (N.V.)

² Department of Engineering, University of Naples Parthenope, 80143 Naples, Italy; francesco.abbondati@uniparthenope.it

* Correspondence: rosa.veropalumbo@unina.it; Tel.: +39-081-768-83379

Abstract: In the road construction sector, the CO₂ emissions that affect global warming are, in most cases, from the asphalt mixtures production activities that are carried out at high temperature (above 160 °C). The research here presented aims to investigate the physical-mechanical properties of asphalt mastics made up using jet grouting waste (JW) as a filler produced through both cold (40–50 °C) and hot mixing process. The first step focused primarily on examining the effects of optimal blending time and curing time of the mastics. The second step focused on the investigation of the rheological properties using a dynamic shear rheometer and carrying out a frequency sweep test at temperatures ranging from 0 to 50 °C with increments of 10 °C, and a multiple stress creep and recovery (MSCR) test under 0.1 and 3.2 kPa load levels at temperatures of 40 and 50 °C. Four cold asphalt mastic solutions were analyzed and then compared to three hot traditional ones, keeping constant, on the one hand, the binder weight and filler over binder weight ratio (0.5), and, on the other hand, changing the type and amount of filler. The compositions of the hot and cold asphalt mastics were as follows: (a) 33% limestone filler (LF) plus 67% bitumen (concerning the cold mixing process, the bitumen content refers to the amount of bitumen into the bitumen emulsion), (b) 33% JW plus 67% bitumen, (c) 16.5% LF plus 16.5% JW and 67% bitumen. The fourth solution designed only for cold asphalt mastic was made up of 33% Portland cement (PC) plus 67% bitumen (referring to the amount of bitumen in the bitumen emulsion). The main findings showed that the optimal performance was achieved at high test temperature by cold and hot asphalt mastics made up adding LF and JW filler, which showed a pronounced elastic behavior. Moreover, the cold asphalt mastic solution made up of LF and JW filler showed better performance than the mastic made up using PC, reaching over 40% increase of the shear modulus and 30% lower non-recoverable creep compliance values at all test temperatures.

Keywords: road asphalt mastics; cold mixing; hot mixing; jet grouting waste; limestone filler; DSR; complex shear modulus; multi stress creep and recovery



Citation: Russo, F.; Veropalumbo, R.; Oreto, C.; Biancardo, S.A.; Abbondati, F.; Viscione, N. Verifying the Mechanical Performance of Cold and Hot Asphalt Mastics Containing Jet Grouting Waste as a Filler. *Coatings* **2021**, *11*, 751. <https://doi.org/10.3390/coatings11070751>

Academic Editor: Filippo Berto

Received: 7 June 2021

Accepted: 21 June 2021

Published: 23 June 2021

Publisher's Note: MDPI stays neutral with regard to jurisdictional claims in published maps and institutional affiliations.



Copyright: © 2021 by the authors. Licensee MDPI, Basel, Switzerland. This article is an open access article distributed under the terms and conditions of the Creative Commons Attribution (CC BY) license (<https://creativecommons.org/licenses/by/4.0/>).

1. Introduction

Climate change can have a direct and indirect impact on the environmental condition that influence road pavement performance. Having to bear the weight of the vehicles and transmit the loads uniformly to the underlying ground, the road pavement is composed of a series of overlapping layers: all these layers should comply with different standards to ensure the safety of users and ease not only the mobility of vehicles, but also future maintenance activities.

From some studies it has been estimated that the construction of a road pavement, due to the uses of main materials, produces on average 7451 t CO₂/km [1] from which heating aggregates, asphalt heating, and mixing process, accounted for 67%, 14%, and

12% of total carbon emissions respectively [2]; for this reason, efforts are being made to reduce CO₂ emissions as much as possible, where some studies [3] have shown that the introduction of innovative road construction technologies reduces of about 84% the CO₂ for maintenance and control of the total road infrastructure.

The upper layers of a flexible pavement are composed of asphalt mixtures.

The asphalt mixture is a temperature-sensitive material; its mechanical characteristics and operational performance dramatically change with temperature variations [4]. The overall performance of an asphalt mixture is significantly influenced by the mechanical properties of the asphalt mastics, which are generally defined as a mixture of binder and mineral filler [5]. Despite the small amount of mineral filler particles in the aggregate size distribution of asphalt mixtures, their surface area takes more than 90% of the total surface area of mineral aggregates [6]. Therefore, the interfacial effect between mineral filler and asphalt binder will significantly affect the performance of asphalt mixture.

Several research studies [7,8] have been carried out on the interfacial interaction between asphalt binder and mineral fillers to find out the factors that influence the interfacial interactions. Temperature and specific surface area of fillers were found to be the two main factors affecting the interfacial interaction between asphalt binder and mineral fillers. The higher the temperature, the stronger the interfacial interaction. Some studies have also quantitatively investigated the contribution of these interactions to the viscoelasticity of asphalt mastics by modelling; Guo and Tan [9], for example, established a correlation between interfacial interactions and viscoelasticity of asphalt mastics by fitting analysis. They found that the interaction degree can be enhanced by elevating the polar components ratio of asphalt binder, increasing the specific surface area of fillers, making the size composition of fillers finer or increasing the temperature.

With the aggravation of environmental and resource consumption problems, a lot of scholars are trying to substitute traditional fillers with marginal materials [10] with the aim of achieving the same or even better mechanical performance than traditional solutions.

Qin et al. [11] studied the impact of basalt fiber (BF) on the physical and mechanical properties of an asphalt mastic. In particular, they conducted a cone penetration test, which was performed by means of a mortar consistency tester with an extra weight of 500 g, to determine the shear behavior of asphalt mastics. The results showed that the properties (asphalt adsorption, strength behavior, crack resistance, and high-temperature rheological properties) of asphalt mastics with the addition of BF improved significantly, especially the crack resistance, when the length and fibers content were respectively equal to 6 mm and in the range 5–7% by the weight of the binder.

Li et al. [12], instead, investigated the feasibility of using the steel slag fillers obtained by different types of basic oxygen furnace in substitution of the traditional limestone filler (LF) for making mastics. An accurate temperature sweep analysis was carried out through a dynamic shear rheometer (DSR) to investigate the rutting potential of asphalt mastics in a fixed-frequency of 10 rad/s in the temperature range 30–60 °C. The results of the study showed that all asphalt mastics containing steel slag fillers show better high-temperature deformation resistance than the mastic with LF; this was due to the stable mastic structure strengthened by the stiffness of steel slag, as well as the chemical interaction between alkaline components in steel slag fillers and asphaltic acid in bitumen.

Wang et al. [13] evaluated the high-temperature and low-temperature properties of asphalt mastics made up of different types of oil shale ash (OSA) as partial replacement of conventional mineral filler using DSR. The results showed that, as the test temperature increased, the asphalt mastics with OSA had lower shear modulus and higher phase angle than traditional asphalt mastics; therefore, it was found that the fluidity of asphalt mastics increased, shifting from elastic to viscous behavior.

Mongkol et al. [14] determined the effect of bagasse and coconut peat fillers on the viscosity and the resistance to failure of asphalt mastics. The findings showed that the viscosity of asphalt mastics with coconut peat and bagasse fillers was relatively similar to that of the traditional LF mastic, and higher than that of the granite filler mastic (at

20% filler content by volume, at all test temperatures); they addressed the results to the shape of the microparticles, which was more rounded for the granite filler particles than the rest of the studied fillers.

Up to date, the recycling of reclaimed asphalt pavement (RAP) in a cold recycled mixture (CRM) with bitumen emulsion (BE) or foamed bitumen is one of the most effective and low-environmental impact technologies [15,16]. The life cycle assessment studies [17] revealed that the CRM technologies reduced the energy consumption by 56–64%, and decreased the greenhouse gas (GHG) emissions by 39–46%.

The properties of CRMs depend on the qualitative and quantitative selection of their components, which are usually RAP, virgin aggregates, BE or foamed bitumen, water, and active filler [18]. Depending on the combination of binding agents, various types of cold recycling mixtures can be distinguished, such as cement-treated materials (CTMs) with cement as the only binding agent, or cement–bitumen-treated materials (CBTMs) containing BE or foamed bitumen with a ratio of residual bitumen to cement (B/C) lower than or equal to one ($B/C \leq 1$).

Few studies have focused on the analysis of cold bituminous mastics made up of filler and BE at mixing temperatures of 40–60 °C.

Li et al. [19] investigated the rheological properties and the microstructure of a mineral filler–asphalt mastic, a mineral filler–residue mastic, and a cement–residue mastic; the results showed that the cement particles do not only act as a filler, but the formation of hydration products in the mastic greatly promotes the increase of the mastic's modulus and elastic properties.

Yinfei et al. [20] analyzed the influence of hollow glass microsphere (HGM) on the performances of asphalt mastic; they found out that the replacement of the traditional LF with HGM could enhance the thermal resistance of the asphalt mastic. In particular, the thermal conductivity of the HGM mastic was about 40% lower, and, at the same time, the non-recoverable creep compliance (J_{nr}) was 50% and 80% lower, respectively at 0.1 and 3.2 kPa (58 °C), than that of LF mastic.

At the present date there are no studies in the literature dealing with an accurate analysis of cold asphalt mastics, especially when alternative materials are introduced in substitution of traditional filler, which is usually used to correct the aggregate size distribution of cold recycled mixtures containing RAP. Therefore, this paper focuses on investigating the influence of jet grouting waste (JW), the dried waste grout expelled together with the extracted soil during ground consolidation works, on the physical-mechanical properties of asphalt mastics obtained through cold (40–50 °C) and hot (160 °C) mixing processes.

Thus, the main objective of this paper is to evaluate the benefits deriving from the re-use of JW, which derives from a water and cement-based fluid mixture, as a filler for preparing cold mastics, aiming to meet, and eventually improve, the mechanical performance of CRMs using cement as a filler.

A total of three cold asphalt mastics and three hot asphalt mastics were blended with LF, JW, and a combination of 50% LF plus 50% JW. In addition, a cold asphalt mastic was mixed with Portland cement (PC).

A graphical summary of the main stages addressed in this research is shown in Figure 1. First, the main properties of the binders, the neat bitumen 50/70 used for making the hot asphalt mastics, the BE adopted for cold asphalt mastics and the PC used as filler for the comparison with JW, were investigated. Simultaneously, the Rigden voids value and the specific gravity of the two fillers, LF and JW, were analyzed. During the asphalt mastic preparation, a viscosity examination was carried out according to EN 13302 [21] to identify the optimum blending time for each of the seven asphalt solutions. After that, the blended asphalt mastics were investigated in terms of the softening point (R&B) and penetration value at two different curing time: (1) Accelerated curing time for three days at 60 °C; (2) long curing time for 28 days at room temperature (about 25 °C). Finally, the rheological properties of the asphalt mastics, for a comprehensive characterization of their viscoelastic

behavior which cannot be derived from conventional tests [22], were investigated through the following tests: (a) Frequency sweep test [23] at test temperatures ranging from 0 to 50 °C with increments of 10 °C; (b) multiple stress creep and recovery (MSCR) test [24] at 0.1 and 3.2 kPa load levels at 40 and 50 °C test temperatures. In particular, in order to compare the performance of the cold asphalt mastic with JW to the cold asphalt mastic made up of PC, all the cold mastics were analyzed rheologically after the long curing protocol.

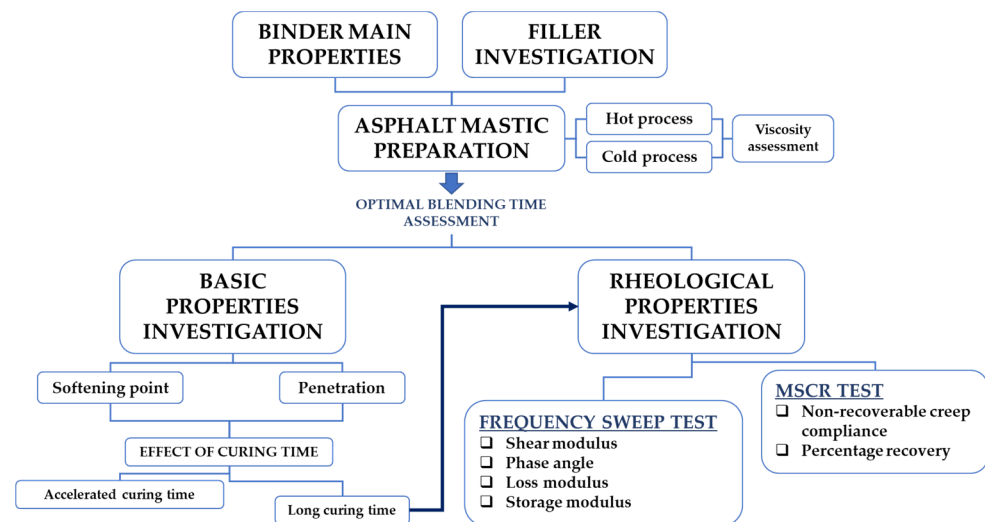


Figure 1. Summary of the main research steps.

2. Materials and Methods

2.1. Materials

2.1.1. Binders

A neat bitumen 50/70 penetration grade (B5070) was adopted for blending the hot asphalt mastics whose main properties are reported in Table 1. A PC 325R and a BE (made up of 40% water and 60% neat bitumen 50/70) were used for the preparation of the cold mastics. The main properties of both the BE and PC are shown in Table 1.

Table 1. Main properties of the binders.

Parameters	Unit	Value	Standard
Bitumen			
Penetration @ 25 °C	dmm	68	EN 1426 [25]
Softening point	°C	46	EN 1427 [26]
Dynamic viscosity @ 150 °C	Pa s	0.25	EN 13702 [27]
Bitumen Emulsion			
Water content	%	40	EN 1428 [28]
pH value	-	4.2	EN 12850 [29]
Settling tendency at 7 days	%	5.8	EN 12847 [30]
Portland Cement			
Initial setting time	min	112	EN 196-3 [31]
Compressive strength	-	-	-
at 2 days	MPa	27.8	EN 196-1 [32]
at 28 days	MPa	61.2	EN 196-1 [32]
Volume constancy	mm	0.52	EN 196-3 [31]

2.1.2. Fillers

The jet grouting waste is the residual material produced during columnar consolidation for the construction of a tunnel. This material, which was poured during the jetting

activity, was conveyed through channels dug into the ground toward a special tank built near the work area, and then subjected to a mechanical dehydration treatment by filter pressing. The residual panel of dehydrated wastewater is the JW. The resulting JW, in solid form, was subjected to a grinding process for 2 h through a jaw mill to obtain traditional filler size (with a passing by mass percentage ranging from 70 to 100 for a sieve size of 0.063 mm, EN 13043 [33]) (see Figure 2).



Figure 2. Limestone filler vs. jet grouting waste as filler.

The chemical composition of the JW filler is reported in Table 2a, where it can be observed that it mainly composes of calcium (25.7%) and silicon (67.64%).

Table 2. Chemical properties of jet grouting waste.

(a)		
Elements	Values	
Ca	25.701%	
Fe	4.859%	
Si	67.642%	
Mg	1.735%	
As	0.003%	
Be	0.003%	
Co	0.004%	
Cr	0.008%	
Ni	0.004%	
Cu	0.007%	
Zn	0.026%	
Others *	0.006%	
* Sn, V, Cd, Ti, Mn		
(b)		
Filler	Specific Gravity (g/cm ³)	Rigden Voids (%)
LF	2.737	41.440
JW	2.687	51.360

The limestone filler, used in this study as control filler, was obtained from the crushing of limestone rock extracted from a quarry located in southern Italy.

The specific gravity and the Rigden voids of LF and JW are reported in Table 2b, where it can be observed that, even if the JW presents a 2% lower specific gravity value than that of LF, the Rigden voids value of the JW resulted 24% higher than that of LF. The stiffening effect of an asphalt mastic is highly dependent on the Rigden voids value: the higher the Rigden voids, the higher the stiffening effect. Therefore, from this preliminary analysis, it

can be stated that the addition of JW to the asphalt binder will result in higher stiffness of the asphalt mastic.

The subsequent analyses presented in this paper were conducted to observe and analyze the effect of JW into cold mastics, where it comes in contact with the water contained in the BE; these effects are compared to those occurring in the hot solutions.

2.1.3. Asphalt Mastic Preparation

In this study, a total of four cold asphalt mastics and three hot asphalt mastics were designed by keeping constant, on the one hand, the bitumen weight (100 g) and the filler over bitumen weight ratio (f/b) to 0.5, and, on the other hand, by changing the filler type as illustrated in Table 3. In particular, the composition of the hot and cold asphalt mastics are as follows: (a) 33% LF plus 67% bitumen (concerning the cold mixing process, the bitumen content refers to the amount of bitumen in the BE), (b) 33% JW plus 67% bitumen, (c) 16.5%LF plus 16.5% JW and 67% bitumen. The fourth solution (see Table 3), designed only as a cold asphalt mastic, was made up of 33% Portland cement (PC) plus 67% bitumen (referring to the amount of bitumen in the BE).

Table 3. Asphalt mastic composition.

ID	f/b	Filler Type	Filler Amount (g)	Binder Type	Binder Amount (g)	Bitumen Amount (g)
HAMJ		JW				
HAML		LF		B5070	100	100
HAMLJ		JW + LF				
CAMC	0.5	PC	50			
CAMJ		JW		BE	167	100
CAML		LF				
CAMLJ		JW + LF				

The preparation of asphalt mastics involved different procedures depending on whether it was a hot or cold asphalt mastic. In both cases, the viscosity check [21] was carried out during the mixing phase (see Figure 3), assuming a total blending time of 800 and 1200 s for the hot and cold asphalt mastics, respectively.

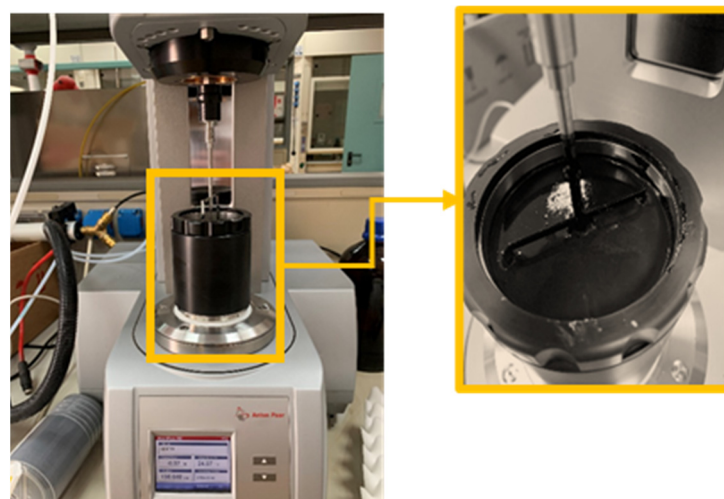


Figure 3. Building material cell equipment (Anton Paar, Graz, Austria) for mixing mastics.

Concerning the preparation of the hot asphalt mastics, the neat bitumen placed into an aluminum container was preheated in the oven at 160 °C and then poured in the cell system until reaching the fixed weight of 100 g. After that, the whole system was kept at 160 °C for 10 min to regulate the temperature. Subsequently, the right amount of filler

(50 g), preheated at 160 °C, was slowly added to the binder and mixed at 2500 rpm; the viscosity was measured during the mixing process.

The viscosity values recorded during the blending phase of the three hot asphalt mastics as a function of time are plotted in Figure 4a. It can be observed that the cold asphalt mastics containing the JW (HAMJ and HAMLJ) required additional 100 s to obtain a constant viscosity value, representative of an homogenous mastic [34], than HAML, which returned an optimum mixing time of 500 s. The final viscosity value of both HAMJ and HAMLJ was on average 33% higher than HAML, which returned the lowest viscosity value, equal to 0.321 Pa·s.

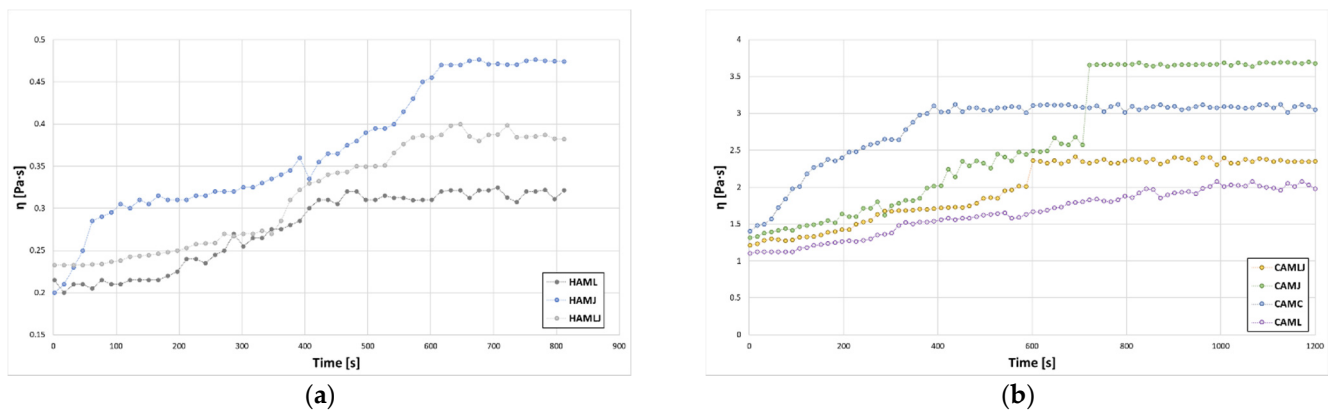


Figure 4. Viscosity vs. blending time: (a) hot asphalt mastics and (b) cold asphalt mastics.

Unlike hot mastics, the preparation of cold mastics was performed at a temperature of 50 °C, which is the maximum working temperature suggested by the manufacturer of the BE used in this study. First of all, the BE was preheated at 50 °C for 1 h in a plastic container (tap), and then poured into the cell system, preheated at the same temperature. The whole system (BE and cell system) was kept at 50 °C for 10 min before starting the mixing process. The filler in the right amount (50 g), previously preheated at 100 °C, was slowly added to the BE and blended at 3500 rpm. The recorded viscosity values for the cold asphalt mastics are reported in Figure 4b. It is interesting to observe how different behaviors have been recorded for each filler: (1) CAML showed a gradual increase of the viscosity over time until reaching a constant value at around 1000 s; (2) CAMC returned an increase of the viscosity up until 400 s, when it reached the constant viscosity value equal to 3.05 Pa·s; (3) CAMLJ exhibited a slight increase of the viscosity until 600 s, after which a sudden rise indicated that the BE broke up; (4) CAMJ showed the breaking up of the BE within 707 s, returning a huge increase in the viscosity value that remained constant until the end of the mixing phase.

The final viscosity value differed for each mastic; in particular, among the cold asphalt mastics, CAML showed the lowest viscosity value equal to 1.98 Pa·s, while CAMJ returned the highest value, equal to 3.67 Pa·s. Looking at the cold asphalt mastic made up of PC, the final viscosity value was 54% and 30% higher than that of CAML and CAMLJ, respectively; on the contrary, CAMC had 17% lower viscosity value than that of CAMJ.

It is worth noting that the addition of JW to both bitumen and bituminous emulsion lead to an increase of the final viscosity of the asphalt mastics.

2.2. Methods

2.2.1. Conventional Properties

The basic properties of hot and cold asphalt mastics were investigated in terms of penetration grade and softening point according to EN 1426 [25] and EN 1427 [26], respectively (see Figure 5a,b).

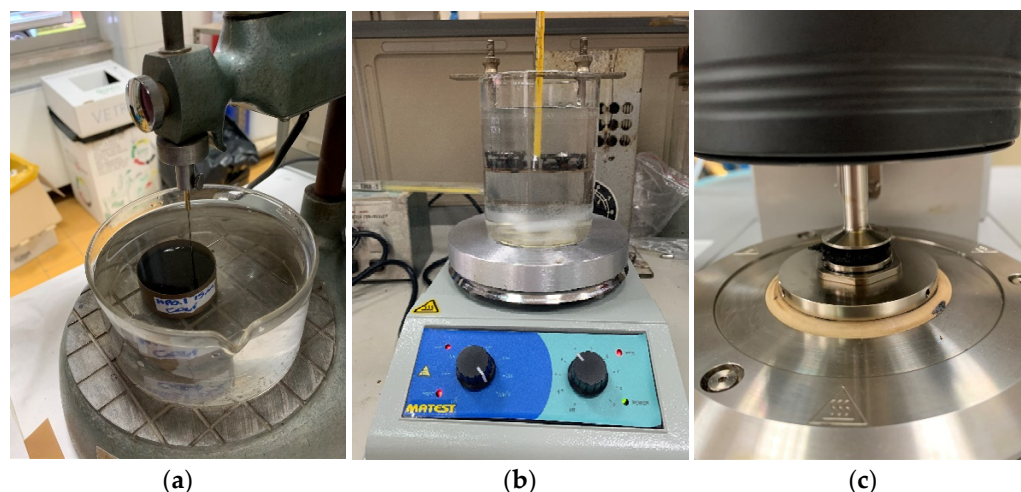


Figure 5. Investigation of the performance of asphalt mastics: (a) penetration device, (b) R&B equipment, and (c) DSR configuration for frequency sweep and MSCR tests.

The penetration index was calculated according to Equation (1) to evaluate the temperature susceptibility of the hot and cold asphalt mastics.

$$\text{Penetration index} = (20 - 500A) / (1 + 50A) \quad (1)$$

where

$$A = (\log \text{penetration}@T - \log 800) / (T - T_{R\&B}) \quad (2)$$

where T is the penetration test temperature ($^{\circ}\text{C}$) and $T_{R\&B}$ is the softening point temperature ($^{\circ}\text{C}$).

2.2.2. Rheological Properties

The frequency sweep test [23] was performed on all the hot and cold asphalt mastics and B5070 using the DSR SmartPave 102 Anton Paar. The test was carried out at 20 frequencies from 0.1 to 10 Hz, and six temperatures in the range 0–50 $^{\circ}\text{C}$, with increments of 10 $^{\circ}\text{C}$.

The DSR configuration consisted in a “25 mm plate-plate geometry” with a 1 mm gap for test temperatures above 30 $^{\circ}\text{C}$ (see Figure 5c), while “8 mm plate-plate geometry” with a 2-mm gap was adopted for test temperatures below 30 $^{\circ}\text{C}$.

The linear viscoelastic (LVE) strain limit for all the asphalt binders at different frequencies and temperatures was measured through the strain sweep test according to standardize procedures [35].

In order to comply with the requirements of the research study, the lowest shear strain sweep value was selected to make an effective comparison of all asphalt mastics as follows: 0.1% for a “25 mm plate-plate geometry” configuration and 0.05% for an “8 mm plate-plate geometry” configuration.

The obtained shear modulus G^* and phase angle δ were plotted in the black diagram space [36]. The storage modulus G' and the loss modulus G'' were analyzed through the Cole-Cole diagram [37].

The MSCR [24] was conducted through the DSR applying ten cycles of repeated creep and recovery with a loading time of 1 s and an unloading time of 9 s at both shear stress levels of 0.1 and 3.2 kPa.

The test was carried out at 40 and 50 $^{\circ}\text{C}$ test temperatures with a “25 mm plate-plate geometry” configuration with 1 mm gap.

The results of the MSCR test are used to characterize the deformation resistance of asphalt mastics through J_{nr} and the percent recovery (%Recovery), calculated by Equations (3) and (4), respectively.

$$J_{nr\tau} = \frac{1}{10} \sum_{N=1}^{10} (\epsilon_{10} / \tau) \text{ (kPa}^{-1}\text{)} \quad (3)$$

$$\% \text{Recovery}_{\tau} = \frac{1}{10} \sum_{N=1}^{10} \left[100 \cdot (\varepsilon_1^N - \varepsilon_{10}^N) / \varepsilon_1^N \right] (\%) \quad (4)$$

where

- ε_{10}^N is the strain value at the end of the recovery phase (after 10 s) of the N-th cycle;
- τ is the applied stress, 0.1 kPa and 3.2 kPa;
- ε_1^N is the strain value at the end of the creep phase (after 1 s) of the N-th cycle;
- ε_{10}^N is the strain value at the end of the recovery phase (after 10 s) of the N-th cycle.

3. Results and Discussions

3.1. Basic Properties

The softening point and penetration values were adopted to investigate the effect of the curing time on the cold asphalt mastics. In particular, a 28 days of curing time at room temperature (about 25 °C) was selected as the long curing time, since after that period more than 90% of the total mechanical strength of PC, contained in the CAMC solution, developed; instead, 3 days of curing time at 60 °C was chosen as the accelerated curing time [38] to ensure a complete evaporation of the water contained in the BE of cold asphalt mastics. Figure 6 shows the R&B values of the four cold asphalt solutions (CAMC, CAMJ, CAML, and CAMLJ). Looking at the R&B values after the accelerated curing time, the lowest value (48 °C) was returned by CAML, while the highest one (56 °C) was observed for CAMC, resulting in 9%, 17%, and 3% higher than that of CAMJ, CAML, and CAMLJ, respectively.

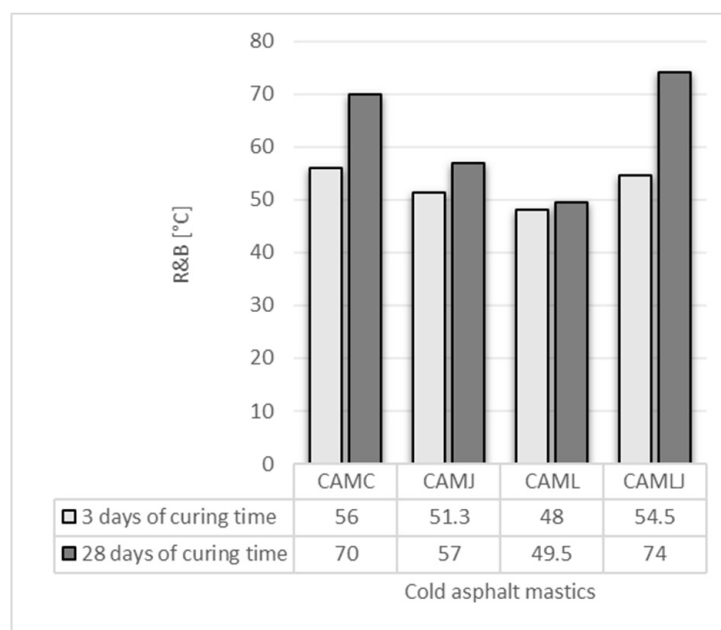


Figure 6. R&B values for cold mastics subjected to different curing time.

Looking at the R&B values after 28 days of curing time, CAML showed again the lowest value (49.5 °C), while the highest value (74 °C) was observed for CAMLJ. In fact, moving from 3 to 28 days of curing time, the mastics CAMC, CAMJ, and CAML increased the R&B value by 25%, 11%, and 3%, while CAMLJ returned 36% higher R&B value.

Different considerations can be drawn for the penetration values (see Figure 7); after the accelerated curing time, the highest value of 67 dmm is obtained by CAMC, while the lowest (62 dmm) is shown by both CAMJ and CAMLJ. As the curing time increases, the penetration values decrease by 33%, 29%, 22%, and 29% for CAMC, CAMJ, CAML, and CAMLJ, respectively. It is interesting to observe that, under the long curing time conditions, the addition of JW to cold asphalt mastics improves the basic performance compared to those of the cold mastic made up with PC.

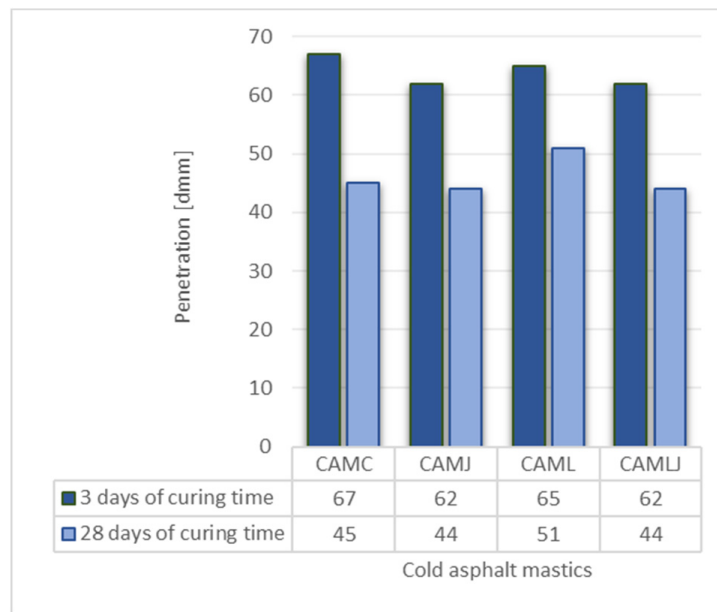


Figure 7. Penetration values for cold mastics subjected to different curing time.

Figure 8 shows the R&B values of the hot asphalt mastics; it can be observed that all the hot asphalt solutions have higher R&B value than B5070. In particular, HAMJ, HAML, and HAMLJ have 24%, 7%, and 35% higher R&B value than that of B5070. Among all, HAMLJ showed the highest R&B value, equal to 62 °C.

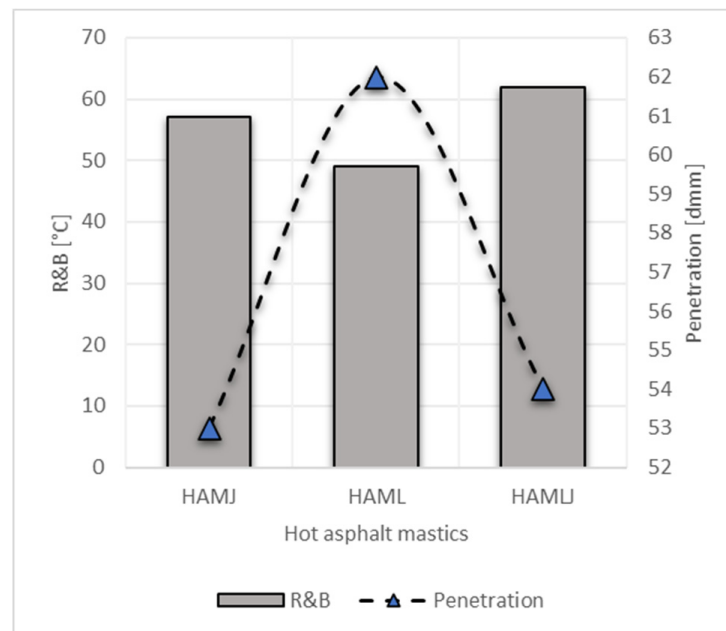


Figure 8. R&B and penetration value of the hot asphalt solutions.

Looking at the comparison of the cold asphalt solutions with the hot ones that have the same filler type and content, all the cold asphalt mastics returned on average 8% lower R&B values than the hot mastics after the accelerated curing time, although they had 11.5% higher R&B values than that of B5070. On the contrary, after the 28 days of long curing time, CAML and CAMJ achieved the same R&B values of HAML and HAMJ, respectively, while CAMLJ had 19% higher R&B value than that of HAMLJ.

The penetration values of the hot asphalt mastics (see Figure 8) are compliant with the R&B values of the same mastics: the highest R&B value corresponds to the lowest

penetration value and vice versa. The lowest penetration value is achieved by HAMJ, which is 2% lower than that of HAMLJ. Again, the penetration values of the hot asphalt solutions are lower (on average 10%) than those obtained by the cold asphalt solutions after the accelerated curing time; instead, when the curing time achieved the 28th day at room temperature, the cold asphalt solutions had on average 18% lower penetration values than those of the hot ones.

The penetration index results are presented in Table 4. As it can be observed, all the mastic solutions containing only LF (both hot and cold) have higher temperature susceptibility than the remaining solutions; instead, when JW is combined with LF, both hot and cold asphalt mastics returned the lowest temperature susceptibility. In fact, CAMLJ (cold solution) and HAMLJ (hot solution) have penetration index values equal to 3.127 and 1.619, respectively. When JW alone is adopted for making mastics, the hot asphalt mastic (HAMJ) has lower temperature susceptibility than the cold one (than CAMJ), with four times higher penetration index value. Anyways, the cold asphalt solution containing PC resulted in the highest penetration index among the remaining asphalt mastics, except for CAMLJ.

Table 4. Penetration index values of the asphalt mastics.

ID	Blending Process	Filler Type	Penetration Index
CAMC		PC	2.559
CAMJ	Hot	JW	0.107
CAML		LF	−1.279
CAMLJ		LF + JW	3.127
HAMJ		JW	0.556
HAML	Cold	LF	−0.947
HAMLJ		LF + JW	1.619

3.2. Frequency Sweep Test

On the basis of the results achieved so far by the basic investigation at different curing time, it was decided to proceed with the rheological investigation of the cold asphalt mastics after the long curing time of 28 days.

The frequency sweep test results were expressed in terms of black diagram by plotting the phase angle versus the shear modulus. A smooth curve in a black diagram is a useful indicator of time–temperature equivalency of the asphalt mastics [39].

Figure 9 shows the black diagrams of the hot asphalt solutions. First of all, it can be observed that all the hot asphalt mastics, regardless of the test temperature, returned higher G^* values (+193% on average) than B5070; moreover, all the solutions investigated present an almost linear trend until G^* value equals 10,000 Pa (see the left portion of the black diagram).

The simultaneous addition of LF and JW resulted in increased stiffness and greater proportion of elastic behavior compared to the other asphalt mastics (HAML and HAMLJ) and the binder B5070. As a matter of fact, HAMLJ presented G^* values between 0 and 20 °C (δ values falling within the range 50–80) on average 121% and 76% higher than that of HAMJ and HAML, respectively; instead HAMLJ had 39% higher G^* than that of HMAL at test temperatures higher than 20 °C, up until matching the G^* value of HMAJ at 50 °C.

No substantial differences in terms of phase angle were returned by the hot asphalt mastics, except for HAMLJ that showed the lowest phase angle (51°) in correspondence of the highest G^* .

The next comparison was carried out among the cold asphalt solutions after 28 days of curing time, as reported in Figure 10. Figure 10 shows that CAMLJ solution had the highest G^* values, in particular seven times higher than those of CAML, which instead exhibited the lowest G^* values.

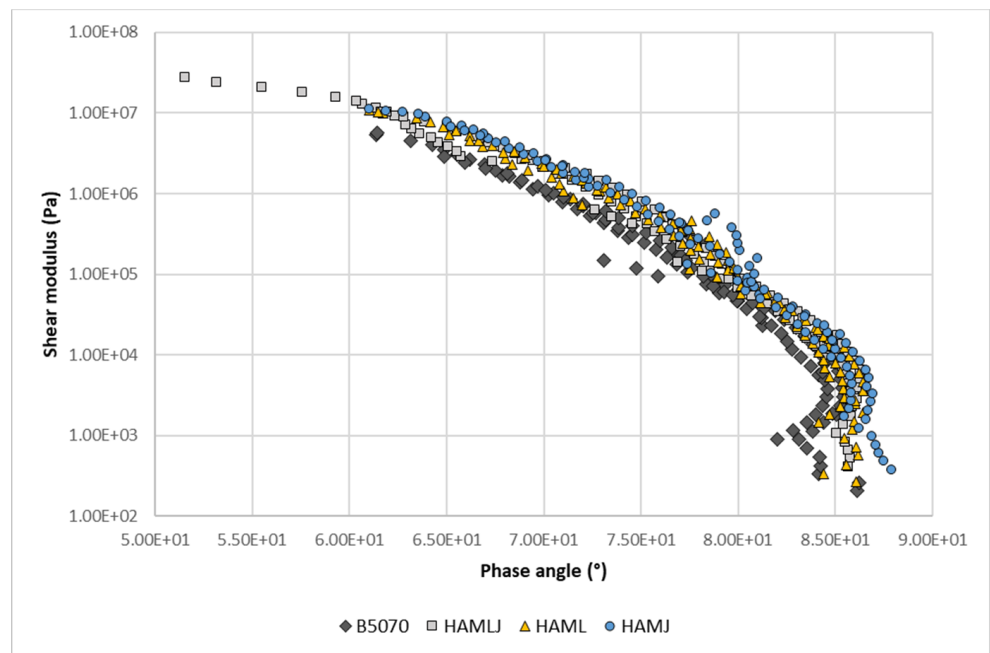


Figure 9. Black diagram comparing the hot asphalt mastics and B5070.

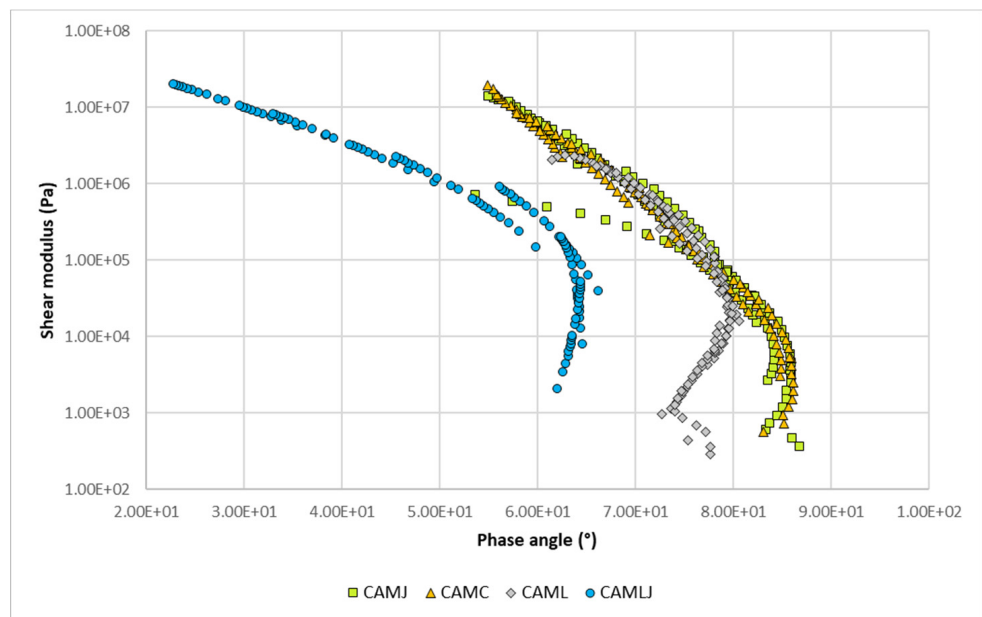


Figure 10. Black diagram comparing the cold asphalt mastics.

When CAMLJ solution is compared to CAMJ, the average G^* value at all test temperatures increases by 82%; the same increase lowers until 40% when comparing CAMLJ to CAMC. At the same time, CAMLJ returned the lowest δ values, in particular lower by 34%, 31% and 30% than those of CAML, CAMJ, and CAMC, respectively.

When the JW is added to cold mastics, no substantial difference is returned in terms of phase angle than CAMC solution. This result favors the hypothesis that the behavior of JW is close to that of PC, given the percentage of cement contained in the JW. Furthermore, it is possible to observe that the linear behavior of the CAMJ and CAMLJ reverses in correspondence of G^* values between 10,000 and 100,000 Pa, before than what has been observed for the corresponding hot asphalt solutions; the drift of the switching point, in

correspondence of which the mastics show a reduction of phase angle values, proves that the cold mastics have a more marked elasticity than the hot ones.

Since the HAMLJ and CAMLJ were the most suitable solutions in terms of G^* and δ among the hot and cold solutions, respectively, further considerations were drawn comparing the two mentioned solutions through the black diagram as reported in Figure 11.

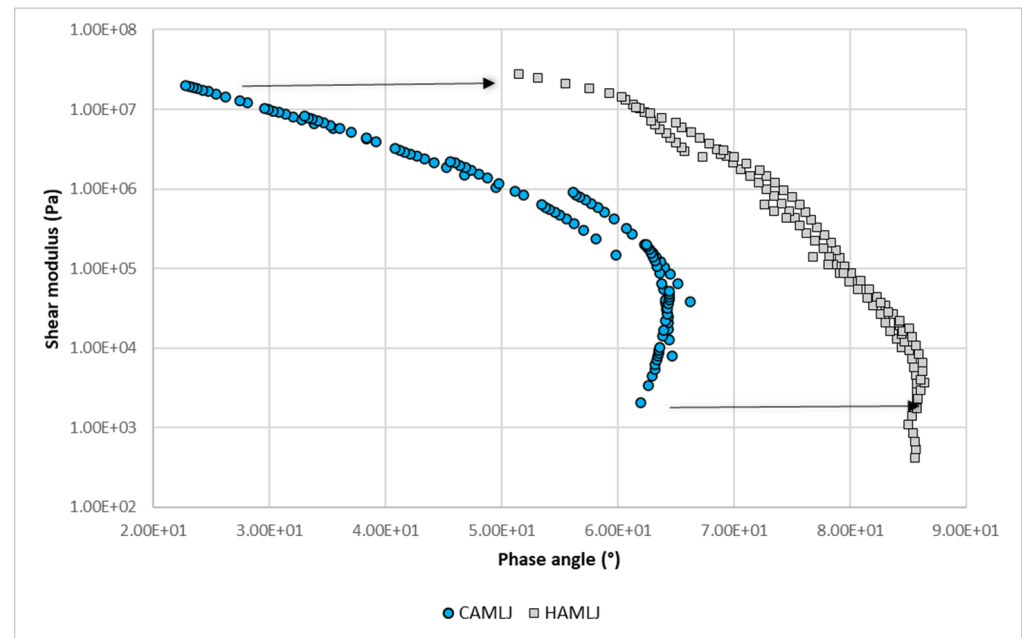


Figure 11. Black diagram of CAMLJ vs. HAMLJ.

What immediately stands out to the eye is that the two curves seem to be offset from one another, with CAMLJ returning the lowest phase angle values for the same G^* values: CAMLJ achieved up to 60% lower phase angle than that of HAMLJ in correspondence of the highest G^* value, while 28% lower phase angle turned out for the lowest G^* value. These results highlighted that the combination of JW and LF into cold mastics returns more elastic solutions, contrary to what has been observed for hot mastics.

Further careful investigations of the performance of the hot mastics, cold mastics, and B5070 were carried out by plotting a Cole-Cole diagram (see Figure 12), where the x-axis indicates the storage modulus (G'), and the y-axis shows the loss modulus (G'') [40] at all test temperatures (from 0 to 50 °C). The CAMLJ and HAMLJ solutions showed a prevalence of the storage modulus over the loss modulus (G' is on average 50% higher than G''), unlike all the other mastics, which presented a predominance of the viscous behavior. The degree of elasticity and viscosity of the cold mastic containing JW (CAMJ) is the same as that of the cold asphalt mastic with PC (CAMC). Moreover, the addition of JW in the cold mastic returns 50% higher increase of G' value than when it is added in the hot asphalt solution (HAMJ), contrary to what happens when using LF.

3.3. Multiple Stress Creep and Recovery

The MSCR test was carried out to measure the permanent deformation of the four cold asphalt mastics (CAMC, CAMJ, CAML, and CAMLJ), the three hot asphalt solutions (HAMJ, HAML, and HAMLJ), and the bitumen (B5070).

Figure 13 shows the results in terms of J_{nr} . All the asphalt mastics showed lower J_{nr} values than that of B5070; in particular, the hot and cold asphalt solutions lowered the J_{nr} by 10% and 80%, respectively, compared to B5070. All the asphalt mastics showed great temperature sensitivity: moving from 40 to 50 °C, the average J_{nr} increase was equal to 205% and 386% under 0.1 and 3.2 kPa stress levels, respectively. The mastics containing JW, regardless of the temperature and the stress level, showed lower J_{nr} values than those of

HAML solution; in particular, HAMJ has 41% and 21% lower J_{nr} values (average values under both stress levels) than those of HAML at 40 and 50 °C, respectively; HAMLJ has 46% and 33% lower J_{nr} values than those of HAML at 40 and 50 °C, respectively. The same occurs when JW is added to cold mastics: CAMJ and CAMLJ show respectively 69% and 84% lower J_{nr} than those of CAML (average values at both test temperatures and stress levels). It is possible to deduce from the obtained results that, regardless of the test temperature and stress level, the cold mastics improve the elasticity compared to the hot ones with the same filler type and content; in fact, the J_{nr} values of CAML, CAMJ, and CAMLJ are on average 59%, 88%, and 97% lower than those of HAML, HAMJ, and HAMLJ, respectively.

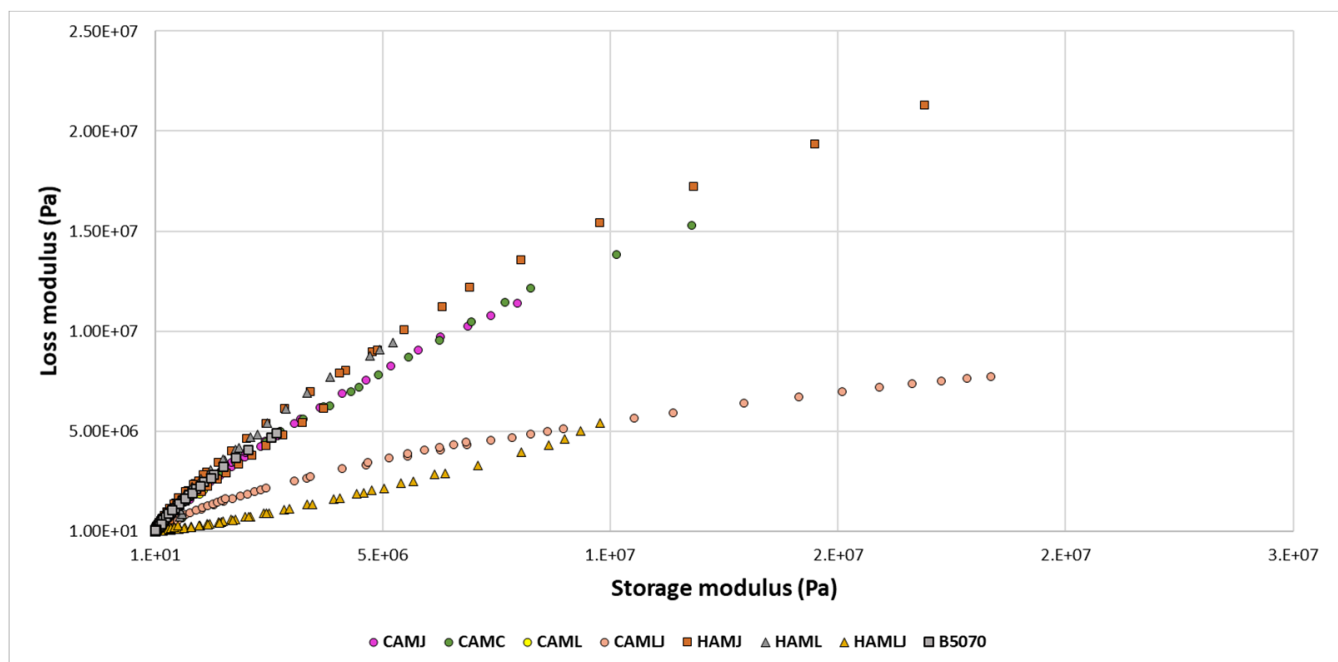


Figure 12. Cole-Cole diagram comparing all asphalt mastics.

Further comparing the CAMC solution to the cold mastics with JW (CAMJ and CAMLJ), two different behaviors are observed, in particular: (1) CAMC shifted from 9% higher average J_{nr} value than that of CAMJ at 40 °C test temperature, to 13% lower J_{nr} at 50 °C; (2) CAMC had always higher J_{nr} values (+140% on average at all test temperatures and stress levels) compared to those of CAMLJ.

The results achieved so far showed that the introduction of JW, in particular when combined with LF into both hot and cold asphalt mastics, helps the binder to resist deformation. The CAMLJ has shown the lowest accumulation of permanent deformation.

In parallel with the non-recoverable creep compliance, the %Recovery was evaluated for the mastic solutions under analysis. Greater %Recovery means greater capacity of an asphalt mastic to recover from the deformation experienced after load application, which translates into lower rutting potential (lower accumulation of plastic deformation) [41,42]. The %Recovery results are reported in Figure 14. It is possible to notice that all asphalt mastic solutions (HAML, HAMJ, HAMLJ, CAML, CAMJ, CAMC, and CAMLJ) returned higher %Recovery than B5070 under both stress levels (0.1 and 3.2 kPa) and test temperatures (40 and 50 °C); in particular, the hot asphalt mastics (HAML, HAMJ, and HAMLJ) showed, on average, five times higher %Recovery than B5070, while cold asphalt mastics had nine times greater %Recovery than B5070. Nevertheless, the asphalt mastics containing only LF (HAML and CAML) returned lower %Recovery than the remaining asphalt solutions; in fact, HAML has on average 63% lower %Recovery than that of both HAMJ and HAMLJ, while CAML has an average 46% lower %Recovery than those of all remaining

cold asphalt solutions. Anyways, all the mastics showed a reduction of the %Recovery moving from 40 to 50 °C, equal on average to 38% and 12% for the hot and the cold solutions, respectively.

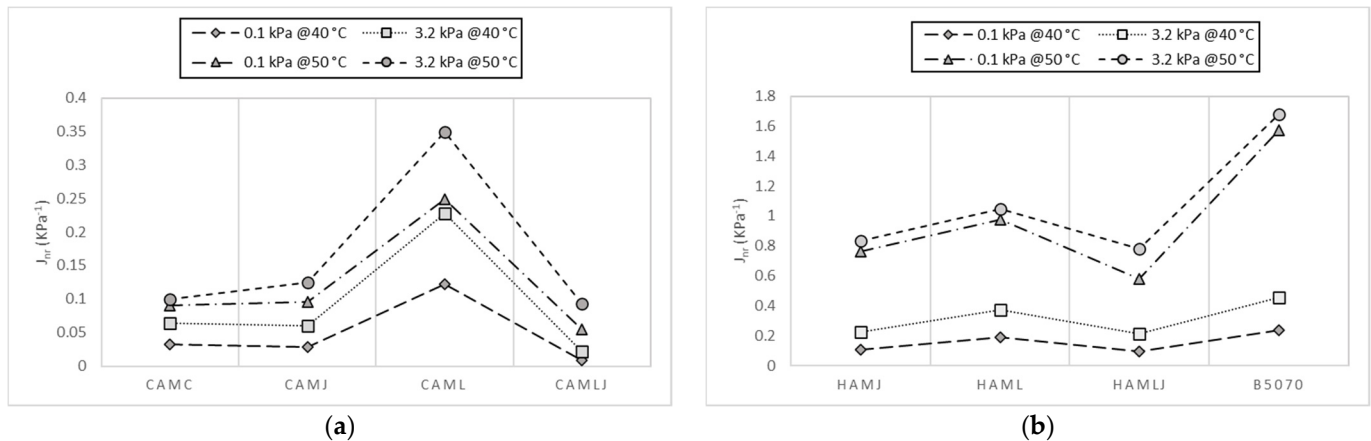


Figure 13. Non-recoverable creep compliance results: (a) cold mastics and (b) hot asphalt mastics and B5070.

Among the hot asphalt solutions, HAMLJ returned the highest %Recovery values, equal to 58%, 52%, 52%, and 51% at 40 °C under 0.1 kPa, at 40 °C under 3.2 kPa, at 50 °C under 0.1 kPa, and at 50 °C under 3.2 kPa, respectively. Compared to those of HAMLJ, CAMLJ returned 34% and 27% higher %Recovery values at 40 and 50 °C (average values at both stress levels), respectively.

The addition of JW seems to improve the deformation recovery properties of the cold mastics more than those of the hot mastics: in fact, CAMJ has on average 63% and 90% higher %Recovery than those of HAMJ under both stress levels at 40 and 50 °C, respectively. Although CAMJ solution is made up of JW, which comprises a portion of cement expelled during land consolidation operations, the solution containing PC still returned 9% higher %Recovery at both test temperatures and stress levels compared to that of CAMJ.

It is interesting to observe that the hot asphalt solution containing both the JW and LF is less stress sensitive than all the other hot mastics; among hot mastics, HAMLJ has the lowest %Recovery decrease moving from 0.1 to 3.2 kPa stress level, equal to 10% and 2% at 40 and 50 °C, respectively; instead, when the JW is added alone for making cold mastics, CAMJ showed the absolute lowest %Recovery decrease moving from 0.1 to 3.2 kPa stress level, equal to 4% and 8% at 40 and 50 °C, respectively.

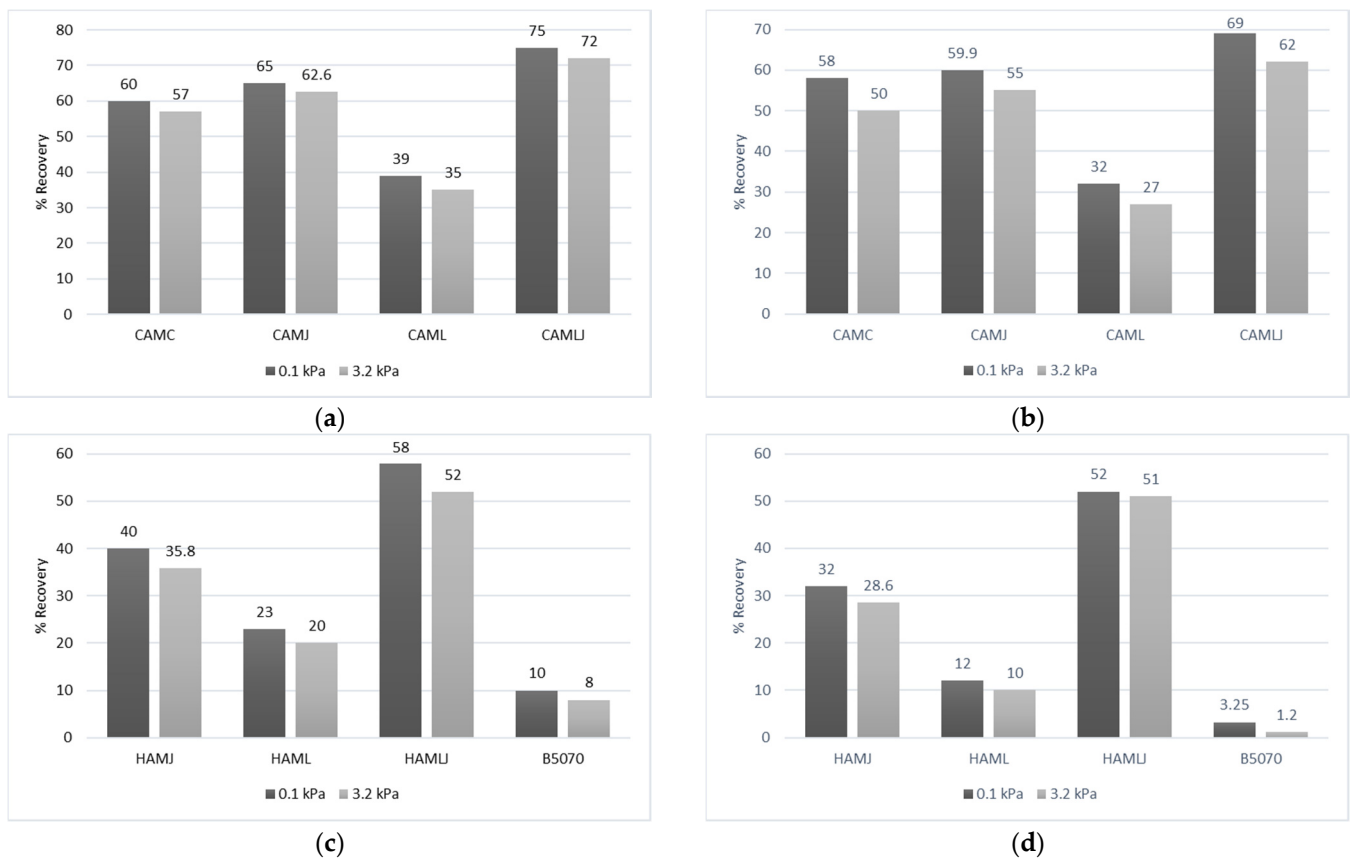


Figure 14. Percent recovery results: (a) cold asphalt mastics at 40 °C, (b) cold asphalt mastics at 50 °C, (c) hot asphalt mastics at 40 °C, and (d) hot asphalt mastics at 50 °C.

4. Conclusions

In this research, the effect of the JW on the properties of asphalt mastics has been investigated. With the aim of reducing the climate change, a deep analysis was carried out on cold asphalt mastics blended with JW at a temperature of 50 °C. The results were compared to the traditional asphalt mastics containing limestone filler (LF) and the main conclusions are as follows:

- The viscosity of the cold mastics is higher than the hot ones and, therefore, the mixing of the cold mastics requires more time than the hot ones (+200 s) to reach a constant viscosity value;
- The analysis of the penetration value and softening point showed that after a curing time of 28 days at room temperature (about 25 °C), the performance of cold mastics increases, exceeding those of the hot ones with the same filler type and content;
- The penetration index values showed that, when the JW is combined with LF into asphalt binders (both through hot and cold blending processes), the asphalt mastics are less temperature susceptible than the remaining analyzed solutions;
- The rheological analysis of the asphalt mastics showed that, after 28 days of curing time, which is usually the time span required to achieve the maximum performance of cement, the mastics made up of JW exceeded the performance of mastics packed with Portland cement (PC), showing 82% higher G^* , and higher elasticity, returning 60% higher %Recovery;
- The combination of JW and LF for making both hot and cold mastics improves the performance of the binder more than all other asphalt solutions analyzed in the present study; at the same, the cold solution with JW and LF returned on average 45% lower phase angle values than the hot one, and, at the same time, five times lower J_{nr} values.

Although the JW is a highly innovative material within road pavements, the results obtained are in line with other studies that involve the reuse of waste as a substitution of traditional filler for making asphalt mastics [43,44]. Furthermore, the addition of JW into asphalt mixtures could save 31% of the CO₂ emission when introduced through a cold process [16].

These results are a starting point for future works that should investigate microscopically the interactions between the limestone filler and the jet grouting waste, which have shown the best performance when combined together. Future studies will also assess the effect of different JW content on the asphalt mastics, focusing on the rheological analysis at low test temperature by evaluating long-term durability of mastics under the loads and temperature impact through the linear amplitude sweep test and evaluating the stiffness modulus through the bending beam rheometer.

Author Contributions: Conceptualization, F.R., R.V. and S.A.B.; methodology, F.R. and R.V.; validation, C.O., F.A. and S.A.B.; formal analysis S.A.B., F.A. and N.V.; investigation, R.V. and N.V.; data curation, F.R., R.V. and C.O.; writing—original draft preparation, F.R., R.V. and S.A.B.; writing—review and editing, R.V., C.O. and S.A.B.; supervision, F.R., F.A. and N.V. All authors have read and agreed to the published version of the manuscript.

Funding: This research received no external funding.

Institutional Review Board Statement: Not applicable.

Informed Consent Statement: Not applicable.

Data Availability Statement: Data available on request due to restrictions eg privacy or ethical.

Conflicts of Interest: The authors declare no conflict of interest.

References

1. Seo, Y.; Kim, S.M. Estimation of materials-induced CO₂ emission from road construction in Korea. *Renew. Sust. Energ. Rev.* **2013**, *26*, 625–631. [\[CrossRef\]](#)
2. Peng, B.; Cai, C.; Yin, G.; Li, W.; Zhan, Y. Evaluation system for CO₂ emission of hot asphalt mixture. *J. Traffic Transp. Eng.* **2015**, *2*, 116–124. [\[CrossRef\]](#)
3. Keijzer, E.E.; Leegwater, G.A.; De Vos-Effting, S.E.; De Wit, M.S. Carbon footprint comparison of innovative techniques in the construction and maintenance of road infrastructure in The Netherlands. *Environ. Sci. Policy* **2015**, *54*, 218–225. [\[CrossRef\]](#)
4. Sun, L. Distribution of the temperature field in a pavement structure. In *Structural Behavior of Asphalt Pavements*; Butterworth-Heinemann: Cambridge, MA, USA, 2016; pp. 61–177.
5. Veropalumbo, R.; Russo, F.; Oretto, C.; Biancardo, S.A.; Zhang, W.; Viscione, N. Verifying laboratory measurement of the performance of hot asphalt mastics containing plastic waste. *Measurement* **2021**, *180*, 109587. [\[CrossRef\]](#)
6. Guo, M.; Tan, Y.; Hou, Y.; Wang, L.; Wang, Y. Improvement of evaluation indicator of interfacial interaction between asphalt binder and mineral fillers. *Constr. Build. Mater.* **2017**, *151*, 236–245. [\[CrossRef\]](#)
7. Li, F.; Yang, Y.; Wang, L. Evaluation of physicochemical interaction between asphalt binder and mineral filler through interfacial adsorbed film thickness. *Constr. Build. Mater.* **2020**, *252*, 119135. [\[CrossRef\]](#)
8. Li, F.; Yang, Y. Experimental investigation on the influence of interfacial effects of limestone and fly ash filler particles in asphalt binder on mastic aging behaviors. *Constr. Build. Mater.* **2021**, *290*, 123184. [\[CrossRef\]](#)
9. Guo, M.; Tan, Y. Interaction between asphalt and mineral fillers and its correlation to mastics' viscoelasticity. *Int. J. Pavement Eng.* **2021**, *22*, 1–10. [\[CrossRef\]](#)
10. Veropalumbo, R.; Viscione, N.; Russo, F. Rheological and mechanical properties of HMA containing fly ashes as alternative filler. In *Proceedings of the International Symposium on Asphalt Pavement & Environment, Padua, Italy, 11–13 September 2019*; Springer: Berlin, Germany, 2019; pp. 88–97. [\[CrossRef\]](#)
11. Qin, X.; Shen, A.; Guo, Y.; Li, Z.; Lv, Z. Characterization of asphalt mastics reinforced with basalt fibers. *Constr. Build. Mater.* **2018**, *159*, 508–516. [\[CrossRef\]](#)
12. Li, C.; Chen, Z.; Wu, S.; Li, B.; Xie, J.; Xiao, Y. Effects of steel slag fillers on the rheological properties of asphalt mastic. *Constr. Build. Mater.* **2017**, *145*, 383–391. [\[CrossRef\]](#)
13. Wang, W.; Cheng, Y.; Tan, G.; Liu, Z.; Shi, C. Laboratory investigation on high-and low-temperature performances of asphalt mastics modified by waste oil shale ash. *J. Mater. Cycles Waste Manag.* **2018**, *20*, 1710–1723. [\[CrossRef\]](#)
14. Mongkol, K.; Chaturabong, P.; Suwannaplay, A. Effect of bagasse and coconut peat fillers on asphalt mixture workability. *Coatings* **2020**, *10*, 1262. [\[CrossRef\]](#)

15. Li, C.; Ouyang, J.; Cao, P.; Shi, J.; Yang, W.; Sha, Y. Effect of rejuvenating agent on the pavement properties of cold recycled mixture with bitumen emulsion. *Coatings* **2021**, *11*, 520. [[CrossRef](#)]
16. Oreto, C.; Veropalumbo, R.; Viscione, N.; Biancardo, S.A.; Russo, F. Investigating the environmental impacts and engineering performance of road asphalt pavement mixtures made up of jet grouting waste and reclaimed asphalt pavement. *Environ. Res.* **2021**, *198*, 111277. [[CrossRef](#)] [[PubMed](#)]
17. Gu, F.; Ma, W.; West, R.C.; Taylor, A.J.; Zhang, Y. Structural performance and sustainability assessment of cold central-plant and in-place recycled asphalt pavements: A case study. *J. Clean. Prod.* **2019**, *208*, 1513–1523. [[CrossRef](#)]
18. Konieczna, K.; Pokorski, P.; Sorociak, W.; Radziszewski, P.; Żymełka, D.; Król, J.B. Study of the stiffness of the bitumen emulsion based cold recycling mixes for road base courses. *Materials* **2020**, *13*, 5473. [[CrossRef](#)]
19. Li, Y.; Lyv, Y.; Fan, L.; Zhang, Y. Effects of cement and emulsified asphalt on properties of mastics and 100% cold recycled asphalt mixtures. *Materials* **2019**, *12*, 754. [[CrossRef](#)]
20. Yinfei, D.; Mingxin, D.; Haibin, D.; Deyi, D.; Peifeng, C.; Cong, M. Incorporating hollow glass microsphere to cool asphalt pavement: Preliminary evaluation of asphalt mastic. *Constr. Build. Mater.* **2020**, *244*, 118380. [[CrossRef](#)]
21. *European Standard. EN 13302. Bitumen and Bituminous Binders—Determination of Dynamic Viscosity of Bituminous Binder Using a Rotating Spindle Apparatus*; European Standard: Brussels, Belgium, 2018.
22. Bahia, H.U.; Anderson, D.A. The new proposed rheological properties of asphalt binders: Why are they required and how do they compare to conventional properties. In *Physical Properties of Asphalt Cement Binders*; ASTM International: West Concord, PA, USA, 1995. [[CrossRef](#)]
23. *European Standard. EN 14770. Bitumen and Bituminous Binders—Determination of Complex Shear Modulus and Phase Angle—Dynamic Shear Rheometer (DSR)*; European Standard: Brussels, Belgium, 2012.
24. *European Standard. EN 16659 Bitumen and Bituminous Binders—Multiple Stress Creep and Recovery Test (MSCRT)*; European Standard: Brussels, Belgium, 2015.
25. *European Standard. EN1426 Bitumen and Bituminous Binders—Determination of Needle Penetration*; European Standard: Brussels, Belgium, 2015.
26. *European Standard. EN 1427 Bitumen and Bituminous Binders—Determination of the Softening Point—Ring and Ball Method*; European Standard: Brussels, Belgium, 2015.
27. *European Standard. EN 13702 Bitumen and Bituminous Binders. Determination of Dynamic Viscosity of Bitumen and Bituminous Binders by the Cone and Plate Method*; European Standard: Brussels, Belgium, 2018.
28. *European Standard. EN 12850 Bitumen and Bituminous Binders—Determination of the pH Value of Bituminous Emulsions*; European Standard: Brussels, Belgium, 2009.
29. *European Standard. EN 12847 Bitumen and Bituminous Binders—Determination of Settling Tendency of Bituminous Emulsions*; European Standard: Brussels, Belgium, 2009.
30. *European Standard. EN 196-3 Methods of Testing Cement. Determination of Setting Times and Soundness*; European Standard: Brussels, Belgium, 2016.
31. *European Standard. EN 196-1 Methods of Testing Cement—Part 1: Determination of Strength*; European Standard: Brussels, Belgium, 2016.
32. *European Standard. EN 1428 Bitumen and Bituminous Binders—Determination of Water Content in Bitumen Emulsions—Azeotropic Distillation Method*; European Standard: Brussels, Belgium, 2012.
33. *European Standard. EN 13043 Aggregates for Bituminous Mixtures and Surface Treatments for Roads, Airfields and Other Trafficked Areas*; European Standard: Brussels, Belgium, 2013.
34. Kuity, A.; Das, A. Homogeneity of filler distribution within asphalt mix—A microscopic study. *Constr. Build. Mater.* **2015**, *95*, 497–505. [[CrossRef](#)]
35. Veropalumbo, R.; Russo, F.; Viscione, N.; Biancardo, S.A.; Oreto, C. Investigating the rheological properties of hot bituminous mastics made up using plastic waste materials as filler. *Constr. Build. Mater.* **2021**, *270*, 121394. [[CrossRef](#)]
36. Rochlani, M.; Leischner, S.; Wareham, D.; Caro, S.; Falla, G.C.; Wellner, F. Investigating the performance-related properties of crumb rubber modified bitumen using rheology-based tests. *Int. J. Pavement Eng.* **2020**, 1–11. [[CrossRef](#)]
37. Angelone, S.; Casaux, M.C.; Zorzutti, L.; Martinez, F. Linear Viscoelastic Properties of a Half Warm Asphalt Mixture (HWMA) with Bitumen Emulsion. In Proceedings of the 9th International Conference on Maintenance and Rehabilitation of Pavements—Mairepav9, Cham, Switzerland, 20 June 2020; Springer: Berlin, Germany, 2020; pp. 507–516. [[CrossRef](#)]
38. Du, S. Effect of curing conditions on properties of cement asphalt emulsion mixture. *Constr. Build. Mater.* **2018**, *164*, 84–93. [[CrossRef](#)]
39. Yang, Q.; Li, X.; Zhang, L.; Qian, Y.; Qi, Y.; Kouhestani, H.S.; Shi, X.; Gui, X.; Wang, D.; Zhong, J. Performance evaluation of bitumen with a homogeneous dispersion of carbon nanotubes. *Carbon* **2020**, *158*, 465–471. [[CrossRef](#)]
40. Carreño Gómez, N.H.; Oeser, M. Investigation on the use of a novel chemical bitumen additive with reclaimed asphalt and at lower mix production and construction temperatures: A case study. *Road Mater. Pavement Des.* **2021**, *22* (Suppl. 1), 641–661. [[CrossRef](#)]
41. D'Angelo, J.; Kluttz, R.; Dongre, R.N.; Stephens, K.; Zanzotto, L. Revision of the superpave high temperature binder specification: The multiple stress creep recovery test (with discussion). *J. Assoc. Asph. Paving Technol.* **2007**, *76*, 123–162.

-
42. Bastos, J.B.; Babadopulos, L.F.; Soares, J.B. Relationship between multiple stress creep recovery (MSCR) binder test results and asphalt concrete rutting resistance in Brazilian roadways. *Constr. Build. Mater.* **2017**, *145*, 20–27. [[CrossRef](#)]
 43. Shirzad, S.; Hassan, M.M.; Aguirre, M.A.; Mohammad, L.N.; Cooper, S., Jr.; Negulescu, I.I. Rheological properties of asphalt binder modified with recycled asphalt materials and light-activated self-healing polymers. *Constr. Build. Mater.* **2019**, *220*, 187–195. [[CrossRef](#)]
 44. Wang, X.; Guo, Y.; Ji, G.; Zhang, Y.; Zhao, J.; Su, H. Effect of biowaste on the high-and low-temperature rheological properties of asphalt binders. *Adv. Civ. Eng.* **2021**, 2021. [[CrossRef](#)]